

## Supplementary Information

### Proton Conductivity of $\text{Li}^+\text{-H}^+$ Exchanged $\text{Li}_7\text{La}_3\text{Zr}_2\text{O}_{12}$ Dense Membranes Prepared by Molten Long-Chain Saturated Fatty Acids

Akihiro Ishii,<sup>\*a</sup> Daisuke Kume,<sup>a</sup> Shoki Nakayasu,<sup>a</sup> Itaru Oikawa,<sup>a</sup> Hiroshi Matsumoto,<sup>b</sup> Hisashi Kato,<sup>b</sup> and Hitoshi Takamura<sup>a</sup>

<sup>a</sup> Department of Materials Science, Graduate School of Engineering, Tohoku University, Sendai 980-8579, Japan.

<sup>b</sup> Research and Development Center, Tohoku Electric Power Co., Inc, Sendai, 980-8550, Japan.

\* Corresponding author email: akihiro.ishii.a4@tohoku.ac.jp

#### S1. Supporting figures

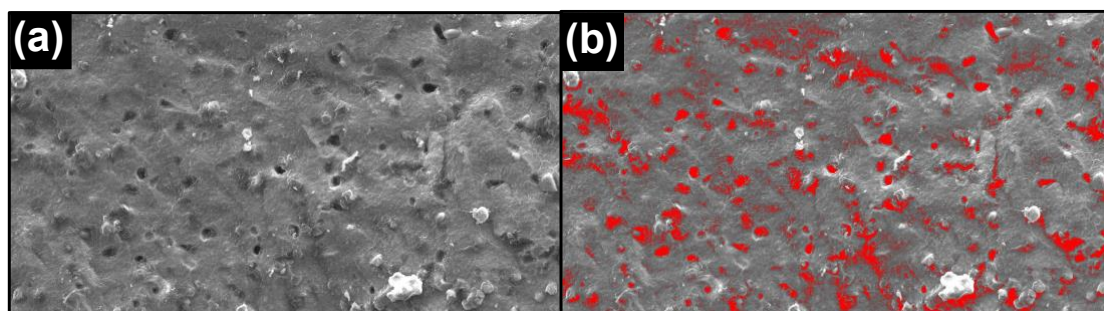


**Fig. S1** (a) Cross-sectional SEM image of LLZ membrane (a part of Fig. 2a in main manuscript), and (b) a result of filling 8% with red color from the dark regions of (a). All the pore regions, along with a small portion of non-void areas, were filled in red. This supports that the relative density of this sample is 92%.

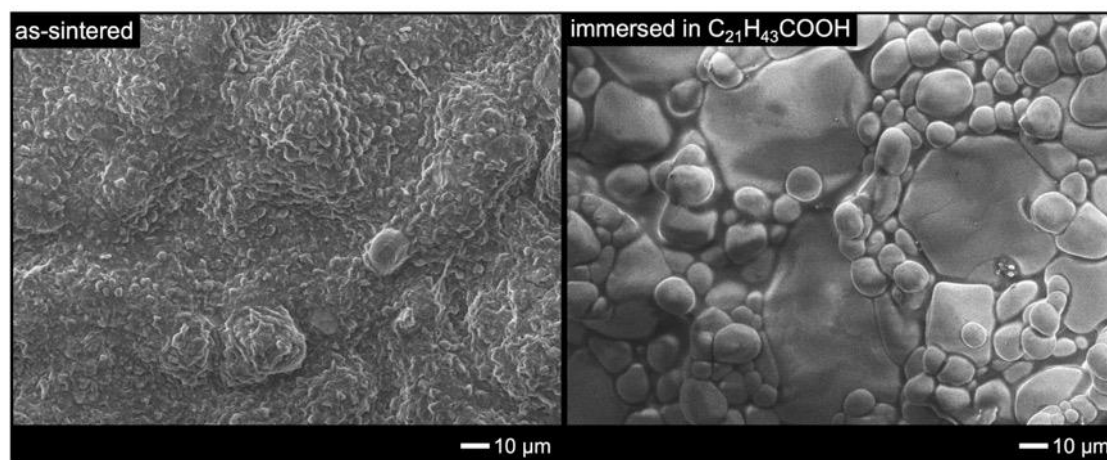


**Fig. S2** Surface SEM images of as-sintered and  $\text{C}_{21}\text{H}_{43}\text{COOH}$ -immersed LLZ membranes.

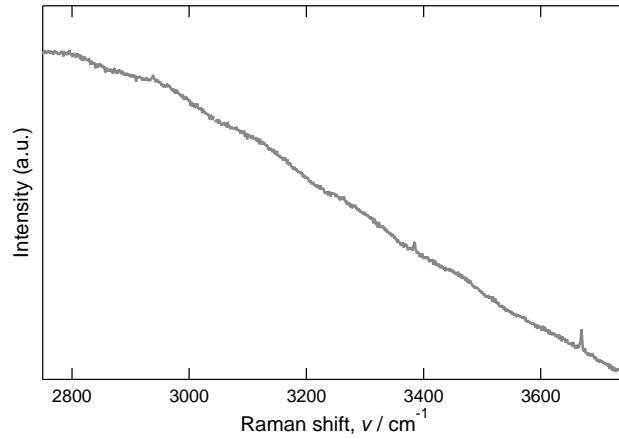


**Fig. S3** Raman spectrum of pristine LLZ dense bodies.

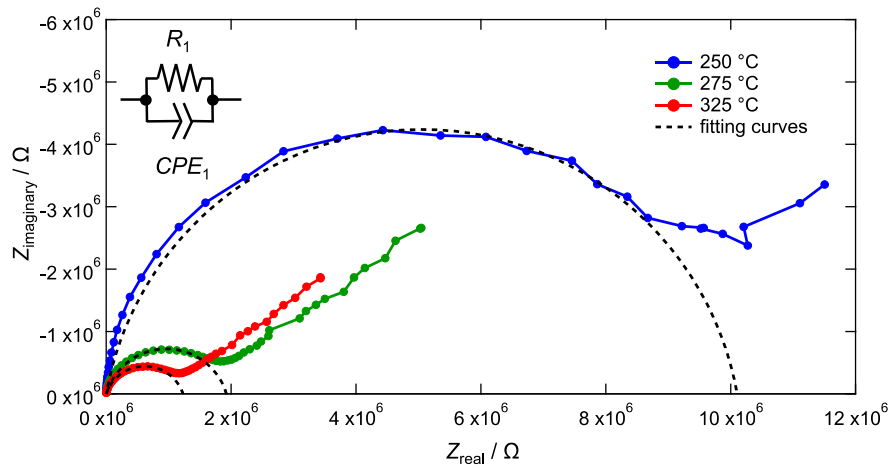


**Fig. S4** Typical Nyquist plot of  $\text{Li}^+\text{-H}^+$  exchanged LLZ dense bodies. The equivalent circuit is also depicted as an inset. The  $p$  value, which is an index of how much the semicircle is distorted ( $p = 1$  corresponds to an ideal semicircle), varied from 0.92 to 0.81 depending on the temperature.

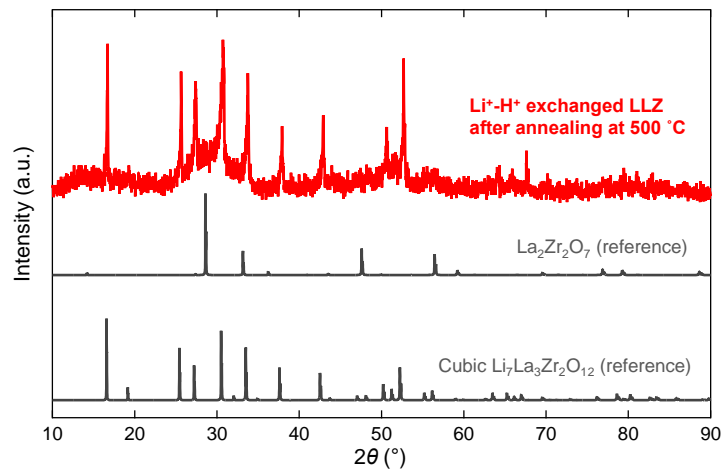


**Fig. S5** XRD pattern of  $\text{Li}^+\text{-H}^+$  exchanged LLZ after annealing at  $500^\circ\text{C}$ . A broad peak is observed around  $28^\circ$  where  $\text{La}_2\text{Zr}_2\text{O}_7$  shows its characteristic peak.

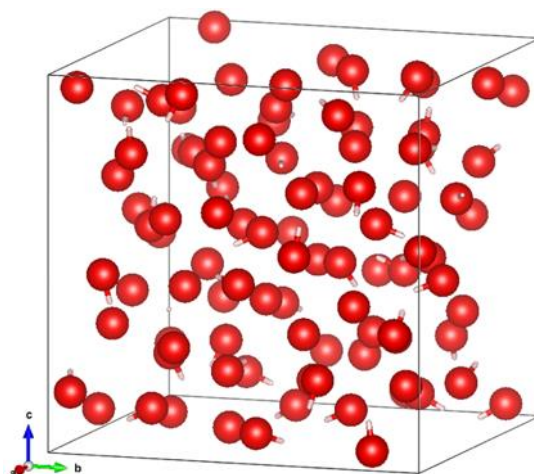


**Fig. S6** Proton distribution in  $\text{Li}^+\text{-H}^+$  exchanged LLZ calculated by DFT-GGA calculation. Elements other than proton (shown in pink) and oxygen (red) are omitted. VESTA [K. Momma and F. Izumi, *J. Appl. Crystallogr.*, **44**, (2011) 1272] was used for visualization.

## **S2. Thermogravimetric analysis to assess stability and water loss of $\text{Li}^+\text{-H}^+$ -exchanged LLZ**

The thermogravimetric analysis was conducted on the LLZ membranes before and after immersion in behenic acid at 250 °C for 15 h, as shown in Fig. S7. The as-sintered LLZ showed 0.4% and 0.9% stepwise weight loss at around 300 °C and at 500 °C, which are attributed to release of  $\text{H}_2\text{O}$  and  $\text{CO}_2$ . [G. Larraz *et al.*, *J. Mater. Chem. A* **1** (2013) 11419-11428] LLZ is sensitive to air exposure, reacting to form  $\text{LiOH}$  in the first step and followed by the reaction to form  $\text{Li}_2\text{CO}_3$ . [Ref. 48 in main manuscript] Meanwhile, the immersed LLZ showed significant weight loss of 6.25 % above 300 °C. Assuming that 1 mol of 91%  $\text{Li}^+\text{-H}^+$  exchanged LLZ ( $\text{H}_{5.61}\text{Li}_{0.55}\text{Al}_{0.28}\text{La}_3\text{Zr}_2\text{O}_{12}$ ) is decomposed by the dehydration reaction (Eq. 3-1 and Eq. 3-2 in main manuscript), it leads to the formation of 2.8 mol of  $\text{H}_2\text{O}$ , which corresponds to 6.24 % of the weight of the  $\text{Li}^+\text{-H}^+$  exchanged LLZ. Thus, this thermogravimetric analysis supports the idea that the decrease in conductivity (shown in Fig. 5 in the main manuscript) is due to the decomposition of the  $\text{Li}^+\text{-H}^+$  exchanged LLZ by the dehydration reaction.

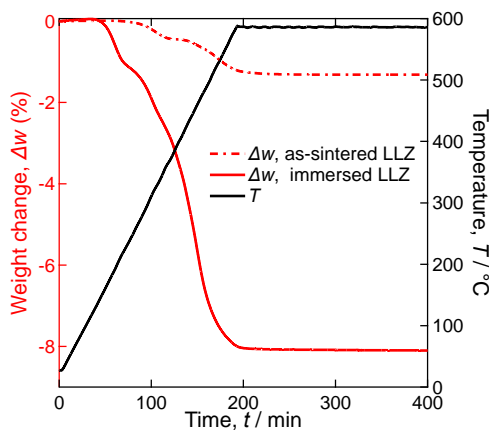


**Fig. S7** Thermogravimetric curves of LLZ membranes before and after immersion in behenic acid at 250 °C for 15 h. Atmosphere was synthetic air and heating ramp was 3 °C·min<sup>-1</sup>.

### S3. Li<sup>+</sup>-H<sup>+</sup> exchange of NASICON-type doped LiZr<sub>2</sub>(PO<sub>4</sub>)<sub>3</sub> by molten long-chain saturated fatty acids

In the same manner as for LLZ, semitransparent NASICON-type Li<sub>1.2</sub>Ca<sub>0.1</sub>Zr<sub>1.9</sub>(PO<sub>4</sub>)<sub>3</sub>-based membranes were prepared, as shown in an inset of Fig. S8a. The samples were not in single phase due to difficulties in phase control, as previously reported [H. El-Shinawi *et al.*, *RSC Adv.* **5** (2015) 17054-17059]. The sample was immersed into molten C<sub>21</sub>H<sub>43</sub>COOH at 270 °C for 40 h; however, no XRD peak shift was observed as shown in Fig. S8a and b. This indicates that no or very limited Li<sup>+</sup>-H<sup>+</sup> exchange was taken place for NASICON-type Li<sub>1.2</sub>Ca<sub>0.1</sub>Zr<sub>1.9</sub>(PO<sub>4</sub>)<sub>3</sub> by this treatment, considering that the lattice constants of LiZr<sub>2</sub>(PO<sub>4</sub>)<sub>3</sub> and HZr<sub>2</sub>(PO<sub>4</sub>)<sub>3</sub> are known to be clearly different [A. Ono, *J. Mater. Sci.* **8** (1984) 1573]. As shown in Fig. S8c, the electrical conductivities of the pristine and C<sub>21</sub>H<sub>43</sub>COOH-immersed samples are almost the same, which supports the limited Li<sup>+</sup>-H<sup>+</sup> exchange for this sample through the immersion into molten C<sub>21</sub>H<sub>43</sub>COOH.

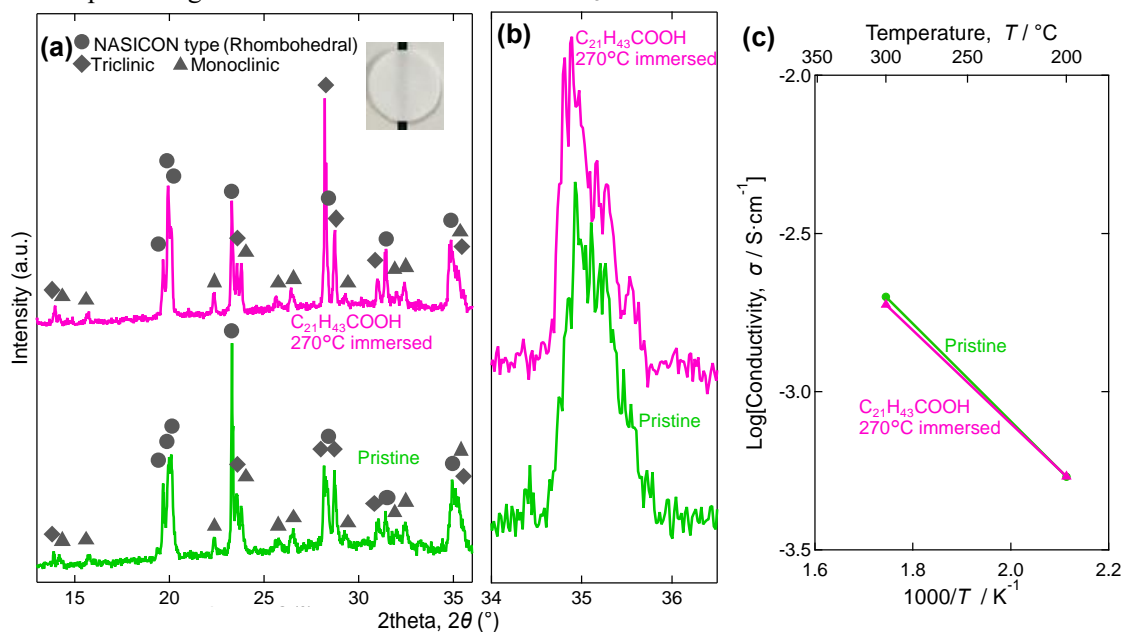


**Fig. S8** (a) XRD patterns of NASICON-type Li<sub>1.2</sub>Ca<sub>0.1</sub>Zr<sub>1.9</sub>(PO<sub>4</sub>)<sub>3</sub>-based membrane before and after the immersion into molten C<sub>21</sub>H<sub>43</sub>COOH heated at 270 °C. Inset is a picture of the Li<sub>1.2</sub>Ca<sub>0.1</sub>Zr<sub>1.9</sub>(PO<sub>4</sub>)<sub>3</sub>-based membrane. (b) Enlarged view of the XRD patterns around 35°. (c) Total electrical conductivity of the NASICON-type Li<sub>1.2</sub>Ca<sub>0.1</sub>Zr<sub>1.9</sub>(PO<sub>4</sub>)<sub>3</sub>-based membrane before and after the immersion.